ChemComm

Accepted Manuscript

This article can be cited before page numbers have been issued, to do this please use: R. Labruere, T. le Saux, L. Jullien, S. Serra, A. Alouane, F. Schmidt, S. Huvelle and R. Plasson, *Chem. Commun.*, 2018, DOI: 10.1039/C8CC03253J.

ROYAL SOCIETY OF CHEMISTRY

rsc.li/chemcomm

View Article Online
DOI: 10.1039/C8CC03253J

ChemComm

COMMUNICATION

A chemically-encoded timer for dual molecular delivery at tailored ranges and concentrations

Received 00th January 20xx,
Accepted 00th January 20xx

DOI: 10.1039/x0xx00000x

Silvia Serra,[a] Ahmed Alouane,[b,c] Thomas Le Saux,[c] Steve Huvelle,[b,c] Raphaël Plasson,[d] Frédéric Schmidt,*[b] Ludovic Jullien*[c] and Raphaël Labruère*[a]

Spatiotemporal control of molecular distribution is much in demand in many fields of Chemistry. To address this goal, we exploit a low molecular weight branched self-immolative architecture, which acts as a triggerable chemically-encoded timer for autonomous sequential release of two chemicals. Using a light-activated model liberating two distinct fluorophores, we generated a tunable spatially contrasted molecular distribution.

Spatial control over molecular organization is often sought for in Chemistry. To address this issue, a first approach exploits sequential deposition of distinct components to yield spatially contrasted solid materials; it most often necessitates a technology and provides frozen molecular organizations.[1] A second approach relies on supramolecular interaction, which is now compatible with targeting molecular organizations both in solids and liquids; processing is facilitated by self-assembly, which further introduces opportunities for triggering structures by means of control parameters (e.g. temperature). More recently, a third approach exploits reaction-diffusion-convection processes in liquids to target dissipative molecular organizations, which exhibit similarities with living matter.[2] With respect to frozen or thermodynamically-driven self-assemblies, the resulting organizations are expected to exhibit a richer behavior since a multitude of processes as well as boundary conditions control their structure at steady-state.[3] However, reaching complex organizations requires the design of molecular components, which exhibit properly tailored rate constants and diffusion coefficients.

Along the latter third approach, we have been recently interested to combine reaction-diffusion processes to target steady-state layered molecular organizations in a liquid. We have introduced a first strategy exploiting a reversible photochemical reaction coupled to proton exchanges which generated singular spatial pH distributions in solutions.[4] We now report on a second strategy, which exploits a molecular timer autonomously liberating substrates after different delays. It builds on a self-immolative precursor, in which the removal of a protective capping moiety after activation with an appropriate stimulus generates a cascade of disassembling reactions in a central spacer ultimately leading to release the substrates.[5] The first released substrates are liberated at higher concentration and over a smaller volume than the later ones. The location and the concentration of each liberated substrate are correspondingly spatially correlated to the position of precursor activation (Figure 1a):[5]

To evaluate our strategy, we adopted a model precursor **cS$_2$(DE/C)** photoreleasing two fluorophores **C** and **D** after activation (Figure 1b).[6,7] **cS$_2$(DE/C)** is made of (i) the 4,5-dimethoxy-2-nitrobenzyl photolabile group (ii) a 2,6-bis(hydroxymethyl)-*p*-cresol core able to release (iii) two latent fluorophores, a coumarin (7-hydroxy-4-(trifluoro-methyl)-2*H*-chromen-2-one) and DDAO (7-hydroxy-9*H*-1,3-dichloro-9,9-dimethylacridin-2-one), which absorb and emit in distinct wavelength ranges and whose emissions are quenched in the precursor with respect to their strongly fluorescent free states. This precursor enabled us to use light for its activation and for independently analyzing the evolution of the concentration of each released fluorophore, as we previously did to analyze the disassembly kinetics of self-immolative spacers.[6]

cS$_2$(DE/C) was synthesized in six steps (see Supporting Information). 2,6-bis(hydroxymethyl)-*p*-cresol mono-oxidation yielded 2-hydroxy-3-(hydroxymethyl)-5-methylbenzaldehyde (82 %),[8] whose Cs_2CO_3-deprotonated phenol group was alkylated with 4,5-dimethoxy-2-nitrobenzyl bromide (88 %). The primary alcohol group was iodinated using a Garegg reaction (55 %). The coumarin was subsequently alkylated with the resulting benzyl iodide in the presence of K_2CO_3 (71 %). The alcohol obtained from reduction of the aldehyde (85 %) was treated with phosgene in anhydrous THF and subsequent addition of DDAO eventually provided **cS$_2$(DE/C)** in 40 % yield.

[a] *Institut de Chimie Moléculaire et des Matériaux d'Orsay (ICMMO), CNRS, Univ Paris Sud, Université Paris-Saclay, 15 rue Georges Clemenceau, 91405 Orsay Cedex, France. E-mail: raphael.labruere@u-psud.fr*
[b] *Institut Curie, PSL Research University Paris, CNRS UMR3666, INSERM U1143, 26, rue d'Ulm, Paris, France. E-mail: Frederic.Schmidt@curie.fr*
[c] *PASTEUR, Département de Chimie, École Normale Supérieure, PSL Research University Paris, Sorbonne Université, CNRS, 75005 Paris, France. E-mail: Ludovic.Jullien@ens.fr*
[d] *Université d'Avignon, UMR 408 Université d'Avignon - INRA, 301 rue Baruch de Spinoza BP 21239, 84916 Avignon Cedex 9, France.*

Electronic Supplementary Information (ESI) available: [Experimental details and supporting figures]. See DOI: 10.1039/x0xx00000x

View Article Online
DOI: 10.1039/C8CC03253J

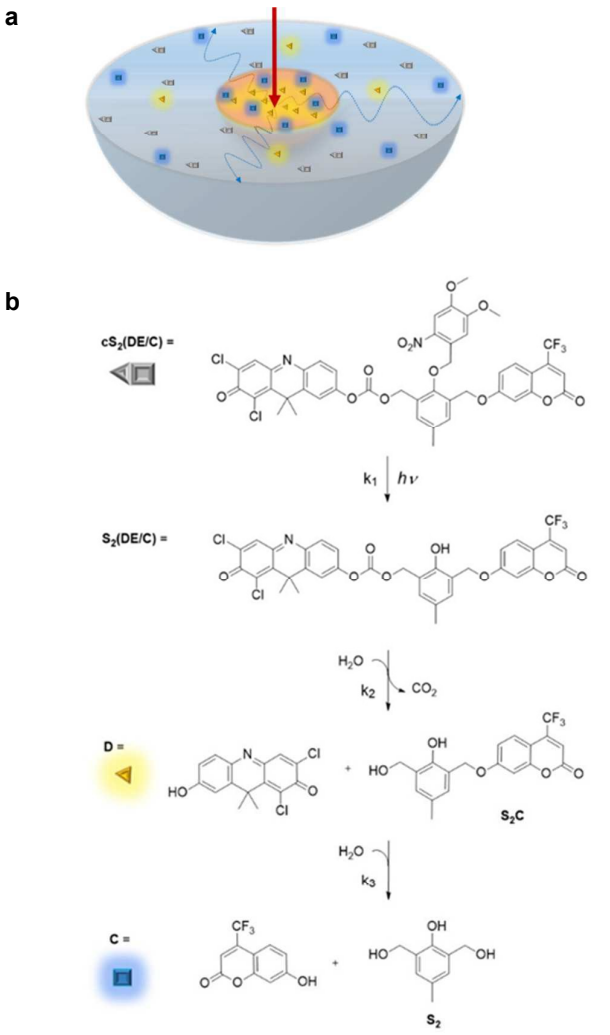

Fig.1 A chemically-encoded timer for temporally-programmed staggered delivery of two substrates with individual control over concentration and space. a) *Concept.* After local activation (red arrow), the self-disassembly of a precursor integrating a low molecular weight architecture acting as a timer liberates autonomously two substrates (displayed as a triangle and a square respectively) after different average delays. After its activation at a locus, the most rapidly liberated substrate (triangle) experiences diffusion for a shorter time and is correspondingly generated in a smaller volume (yellow sphere) and at higher concentration than the most slowly released substrate (square) whose liberation occurs in a larger volume (blue sphere). b) *Reduced kinetic scheme of activation and self-immolation of the model precursor* **cS$_2$(DE/C)**. UV-illumination removes the 4,5-dimethoxy-2-nitrobenzyl photolabile protecting group. A cascade of internal reactions subsequently occurs. It first leads to release the DDAO (**D**) fluorophore together with carbon dioxide. The coumarin (**C**) fluorophore is then liberated together with the benzenic core **S$_2$**.

After preliminarily experiments showing that **cS$_2$(DE/C)** was stable in 1/1 acetonitrile/pH 8 buffer (v/v) at 293 K in the dark for up to 24 h, we first carried out UV-illumination cuvette experiments to analyze its self-immolation kinetics. We recorded the temporal evolution of the fluorescence signals in the emission channels of **C** and **D** from **cS$_2$(DE/C)** solutions undergoing continuous illumination at 365 nm at various light intensities (Figures 2a and b). To analyze the fluorescence increase, we used a reduced kinetic model shown in Figure 1b, which includes the steps occurring beyond a millisecond:[5a,9] **cS$_2$(DE/C)** UV-illumination first affords the phenol intermediate **S$_2$(DE/C)** (rate constant k_1). Based on our previous results,[6] **S$_2$(DE/C)** subsequently disassembles to liberate the phenol-coumarine conjugate **S$_2$C** and the fluorophore **D** (rate constant k_2). Then **S$_2$C** liberates the second fluorophore **C** together with the benzenic core **S$_2$** (rate constant k_3). Satisfactory fits (see Figure 2 and Supporting Information) yielded $k_1 \approx 150I$ Ein^{-1}.m^2 (I designates the surfacic light flux), $k_2 = 40\pm10\ 10^{-3}$ s^{-1}, and $k_3 = 2\pm1\ 10^{-3}$ s^{-1}, in line with our previously reported values for analogous monobranched precursors for which we found $k_1 = 50I$ Ein^{-1}.m^2, $k_2 = 160\ 10^{-3}$ s^{-1}, and $k_3 = 1\ 10^{-3}$ s^{-1}.[10] At light intensity making **cS$_2$(DE/C)** activation non-rate limiting, **D** liberation would be twenty times faster than the **C** one, which already ascertained the potential of the proposed platform for the sequential temporal delivery of two substrates.

To further evaluate our strategy, we then added a spatial dimension to the preceding cuvette experiments. We imaged the fluorescence signals in the **C**- and **D**-emissive fluorescence channels after applying a one-dimensional Gaussian 375 nm light profile for 5 s on a 20 µM **cS$_2$(DE/C)** solution in 4.5/4.5/1 acetonitrile/Britton pH 8 buffer/glycerol (to decrease diffusion coefficients and make easier microscope observation) (v/v/v) sandwiched between two glass plates. The fluorescence signals exhibited spatially contrasted spreading (Figures 2b and e) in fair agreement with numerical simulations exploiting the data obtained in the cuvette experiments (Figures 2c and f; see also Figures 2Sa and b in the Supporting Information). By fixing $k_1 \approx 150I$ Ein^{-1}.m^2 during 375 nm illumination, we extracted $k_2 = 110\ 10^{-3}$ s^{-1} and $k_3 = 2.4\ 10^{-3}$ s^{-1} by using 1.5-3 10^{-10} m^2.s^{-1} for the diffusion coefficients (see Supporting Information).

Such a satisfactory agreement led us to perform simulations to draw the scope of our strategy for generating layered molecular organizations. We adopted a spherical geometry in which the **cS$_2$(DE/C)**-like precursor was activated within a sphere of $\mathcal{R}$ radius upon maintaining constant its concentration at c_0 far from the activation locus; both substrates **C** and **D** were considered to be released in three dimensions with a constant diffusion coefficient $\mathcal{D}$. In this geometry, steady-state concentration profiles not evolving in time are eventually established (see Supporting Information). We explored a large range of values for k_1, k_2, and k_3 in line with the diversity of activation modes (vide infra) and with the tunability of the rate constants associated to disassembly of self-immolative **S$_2$(DE/C)**-like motifs by introducing electron donating or withdrawing groups on the central spacer.[5a,10,11]

C and **D** concentration profiles are governed by k_1-k_3 and by $\mathcal{D}$ and $\mathcal{R}$, which both enter in the scaling rate $k_d = \mathcal{D}/\mathcal{R}^2$. Figures 3a-f display the dependence of the maximal concentrations, D_{max} and C_{max}, (encountered at the activation site) and the widths at half height of the concentration profiles, h_D and h_C, in **D** and **C** resulting from activation of **cS$_2$(DE/C)**-like timers by varying k_1-k_3. The concentrations profiles of the primary product **D** are analyzed in Fig.3a-d. When k_1 and k_2 are larger than k_d, high **D** concentrations (up to c_0) are obtained with h_D in the $\mathcal{R}$ range and a concentration profile with an hyperbolic spatial decay from the activation zone. When k_1 decreases to

View Article Online
DOI: 10.1039/C8CC03253J

ChemComm

COMMUNICATION

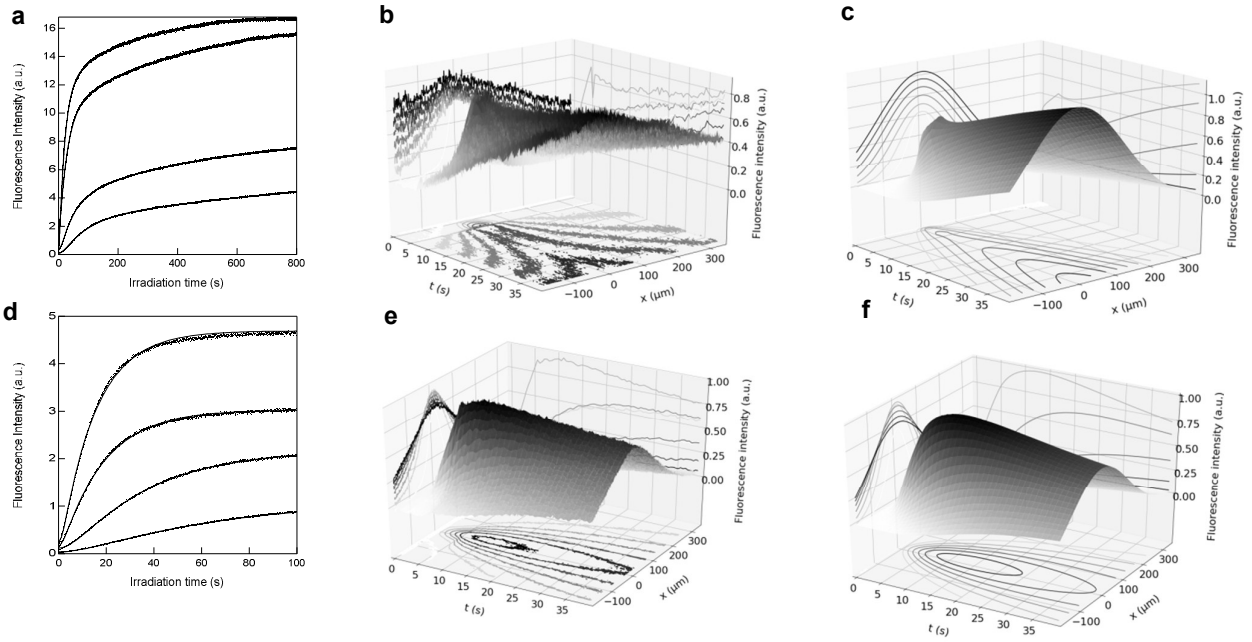

Fig.2 Kinetic analysis of the **cS$_2$(DE/C)** timer. a,d) *Cuvette experiments*. Temporal evolution of the fluorescence emissions $I_F^D(t)$ (a; λ_{exc} = 365 and 645 nm, λ_{em}=660 nm) and $I_F^C(t)$ (d; λ_{exc} = 365 nm, λ_{em} = 500 nm) upon illuminating a 2 µM **cS$_2$(DE/C)** solution at various λ_{exc}=365 nm light intensities (7.1, 14.2, 28.3, and 42.5; in 10^{-4} Ein.m^{-2}.s^{-1}). Dots: experimental data; solid lines: fits with Eq.(17) (a) and (18) (d) in the Supporting Information. Solvent: CH_3CN/0.1 M Britton-Robinson pH 8 buffer 1:1 (v:v); T = 298 K; b,c,e,f) *Fluorescence microscopy*. Temporal evolution of the experimental (b,e) and simulated (c,f) fluorescence signals recorded in the **D** (b,c) and **C** (e,f) emission channels; the first channel reflects the evolution of the sole **D** concentration, while concentrations in **C**, **S$_2$(DE/C)** and **S$_2$C** must be taken into account in the second one. Solvent: 4.5/4.5/1 acetonitrile/Britton pH 8 buffer/glycerol (v/v/v); T = 293 K.

values close to k_d, h_D is conserved but D_{max} drops. In contrast, when k_2 decreases to values close to k_d, D_{max} decreases while h_D widens. When either k_1 or k_2 are much smaller than k_d, D_{max} vanishes to zero. The concentrations profiles of the secondary product **C** are examined in Fig.3e-f. As for **D**, high **C** concentrations (C_{max} up to c_0, h_C in the $\mathcal{R}$ range, hyperbolic spatial decay) are obtained when k_2 and k_3 are larger than k_d. Except in the latter regime, the **C** concentration profile is wider than the **D** one with C_{max} lower than D_{max}, which is particularly pronounced when $k_2 > k_3$. k_2 and k_3 now play symmetrical roles for the **C** production: when either k_2 or k_3 decrease to values close to k_d, C_{max} drops while h_C widens. Eventually, C_{max} vanishes to zero when either k_2 or k_3 is much smaller than k_d.

The preceding simulations point on optimal conditions to generate a layered molecular organization. To avoid using an excessively large **cS$_2$(DE/C)** precursor concentration, one should first fulfill $k_1 >> k_d$. To get contrast in the concentration profiles of **D** and **C**, one should then adopt $k_d > k_2 > k_3$ and adjust the precursor concentration c_0 to get the desired values of D_{max} and C_{max} at the activation locus.

The present strategy could find interesting developments in combination therapies, where multilayered-based macromolecular Drug Delivery Systems[12] lack accurate control over the spatio-temporal delivery aspects of several drugs, even with stimuli-responsive architectures.[13] Hence, in addition to exploiting photoactivation for delivering substrate with light, a **cS$_2$(DE/C)**-like timer could be enzymatically activated to deliver at steady-state two pharmaceutical agents at distinct concentrations in concentric zones of different spatial extension. As a significant example, solid tumors exhibit an inner core of hypoxic cells (often resistant and occupying a volume 5-20 times smaller than the global tumor), surrounded by a shell of normoxic cells at the immediate vicinity, and an external layer of vasculature.[14] Using 1 s^{-1} for k_1 (in the range for activation by the overexpressed protease Cathepsine B at tumor sites[15]) and the present values of k_2 = 110 10^{-3} s^{-1} and k_3 = 2.4 10^{-3} s^{-1} and using 2 10^{-10} m^2.s^{-1} for the diffusion coefficients, we derived 6.8 10^{-3}, 1.2 10^{-4}, 5.1, and 10.7 for D_{max}/c_0, C_{max}/c_0, $h_D/\mathcal{R}$, and $h_C/\mathcal{R}$ with $\mathcal{R}$ = 10 µm. The values 0.66, 2.6 10^{-2}, 1.2, and 1.4 are respectively obtained when $\mathcal{R}$ = 100 µm. The preceding derivation clearly underlines the significance of the boundary conditions on dual delivery: at given **cS$_2$(DE/C)** concentration, a small zone would release large concentrations of **D** and **C** with poor spatial contrast,

View Article Online
DOI: 10.1039/C8CC03253J

whereas a large one would deliver lower but contrasted concentrations of **D** and **C**. Hence we exemplified the relevance of a self-immolative chemically-encoded timer sequentially releasing two chemicals to generate steady-state layered molecular organizations in a liquid. Using a model liberating fluorophores, we demonstrated that the investigated timer could release the first substrate twenty times faster than the second one at the 10-500 s timescale so as to be relevant to yield contrasted spatial organizations at the 100 µm range. Since the rate constants of the self-immolative motif could be tuned by predictable alterations of its structure, various kinetically-governed molecular organizations could be obtained as shown by numerical simulations so as to find a great variety of applications ranging from chemical biology to material science.

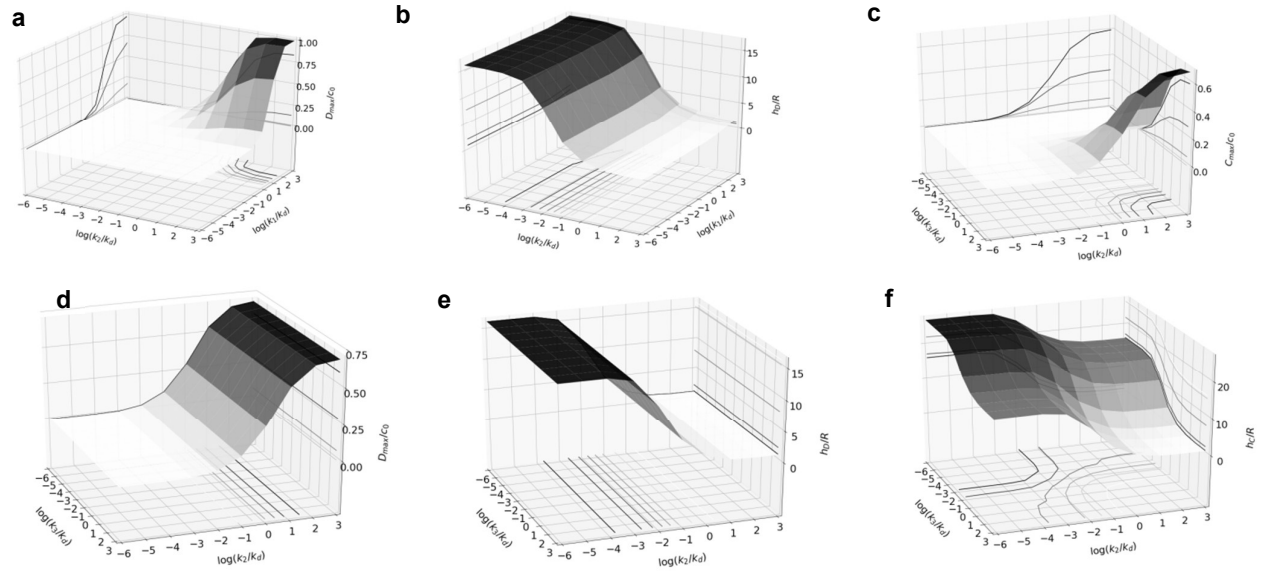

Fig. 3 Tunability of **cS$_2$(DE/C)**-like timers for dual delivery of molecules at tailored range and concentrations. Dependence of the normalized maximal value D_{max}/c_0 and C_{max}/c_0 and of the relative width at half height $h_D/\mathcal{R}$ and $h_C/\mathcal{R}$ of the concentration profiles in **C** and **D** resulting from activation of **cS$_2$(DE/C)**-like timers by varying k_1-k_3. a,b) k_3 = 1 s^{-1} and k_1, k_2 in the [10^{-7}-10^{2}]s^{-1} range, c-f) k_1 = 1 s^{-1} and k_2, k_3 in the [10^{-7}-10^{2}]s^{-1} range. Parameter values: $\mathcal{R}$ = 0.1 mm, $\mathcal{D}$ = 10^{-9} m^2.s^{-1}; k_d = 0.1 s

This work was supported by the ANR Kituse, INSERM (Photocancer project) and LabEx LERMIT. S.S. is a "Ligue Nationale Contre le Cancer" postdoctoral fellow.

Notes and references

1 J. D. Wuest, *Chem. Commun.*, 2005, 5830-5837.
2 S. Soh, M. Byrska, K. Kandere-Grzybowska, B. A. Grzybowski, *Angew. Chem. Int. Ed.,* 2010, **49**, 4170-4198; *Angew. Chem.,* 2010, **122**, 4264-4294.
3 T. Le Saux, R. Plasson, L. Jullien, *Chem. Commun.*, 2014, **50**, 6189-6195.
4 M. Emond, T. Le Saux, J.-F. Allemand, P. Pelupessy, R. Plasson, L. Jullien, *Chem. Eur. J.*, 2012, **18**, 14375-14383.
5 (*a*) A. Alouane, R. Labruère, T. Le Saux, F. Schmidt, L. Jullien, *Angew. Chem. Int. Ed.,* 2015, **54**, 7492-7509; *Angew. Chem.,* 2015, **127**, 7600-7619; (*b*) M. E. Roth, O. Green, S. Gnaim, D. Shabat, *Chem. Rev.,* 2016, **116**, 1309-1352.
6 R. Labruère, A. Alouane, T. Le Saux, I. Aujard, P. Pelupessy, A. Gautier, S. Dubruille, F. Schmidt, L. Jullien, *Angew. Chem. Int. Ed.,* 2012, **51**, 9344-9347; *Angew. Chem.,* 2012, **124**, 9478-9481.
7 (*a*) A. Chaudhuri, Y. Venkatesh, K. K. Behara, N. D. P. Singh, *Org. Lett.,* 2017, **19**, 1598‑1601; (*b*) P. T. Wong, S. Tang, J. Cannon, J. Mukherjee, D. Isham, K. Gam, M. Payne, S. A. Yanik, J. R. Baker, S. K. Choi, *ChemBioChem,* 2017, **18**, 126‑135.
8 R.-G. Xie, Z.-J. Zhang, J.-M. Yan, D.-Q. Yuan, *Synth. Commun.,* 1994, **24**, 53-58.
9 (*a*) M. Caplow, *J. Am. Chem. Soc.,* 1968, **90**, 6795-6803; (*b*) S. L. Johnson, D. L. Morrison, *J. Am. Chem. Soc.,* 1972, **94**, 1323-1334.
10 A. Alouane, R. Labruère, T. Le Saux, I. Aujard, S. Dubruille, F. Schmidt, L. Jullien, *Chem. Eur. J.,* 2013, **19**, 11717-11724.
11 (*a*) A. Alouane, R. Labruère, K. J. Silvestre, T. Le Saux, F. Schmidt, L. Jullien, *Chem. Asian J.,* 2014, **9**, 1334-1340; (*b*) K. M. Schmid, L. Jensen, S. T. Phillips, *J. Org. Chem.,* 2012, **77**, 4363-4374.
12 (*a*) T. Okuda, K. Tominaga, S. Kidoaki, *J. Control. Release,* 2010, **143**, 258-264; (*b*) Z. Zhang, S. Liu, Y. Qi, D. Zhou, Z. Xie, X. Jing, X. Chen, Y. Huang, *J. Control. Release,* 2016, **235**, 125-133; (*c*) W. Xiao, X. Zeng, H. Lin, K. Han, H.-Z. Jia, X.-Z. Zhang, *Chem. Commun.,* 2015, **51**, 1475-1478; (*d*) L. Fan, B. Jin, S. Zhang, C. Song, Q. Li, *Nanoscale*, 2016, **8**, 12553-12559.
13 (*a*) F. Meng, Z. Zhong, J. Feijen, *Biomacromolecules,* 2009, **10**, 197-209; (*b*) C. A. Blencowe, A. T. Russell, F. Greco, W. Hayes, D. W. Thornthwaite, *Polym. Chem.,* 2011, **2**, 773-790; (*c*) T. Ramasamy, H. B. Ruttala, B. Gupta, B. K. Poudel, H.-G. Choi, C. S. Yong, J. O. Kim, *J. Control. Release,* **2017**, **258**, 226-253.
14 (*a*) M. C. Hogan, O. Mathieu-Costello, D. C. Poole, P. D. Wagner in Oxygen Transport to Tissue XVI, Plenum Press, New York, 1994; (*b*) J. C. Forster, W. M. Harriss-Phillips, M. J. J. Douglass, E. Bezak, *Hypoxia (Auckl).,* 2017, **5**, 21-32.
15 (*a*) M. A. Chowdhury, I. A. Moya, S. Bhilocha, C. C. McMillan, B. G. Vigliarolo, I. Zehbe, C. P. Phenix, *J. Med. Chem.,* **57**, 6092-6104; (*b*) B. Gikanga, N. S. Adeniji, T. W. Patapoff, H.-W. Chih, L. Yi, *Bioconjugate Chem.,* **27**, 1040-1049.